

Glycerol-assisted solution combustion synthesis of improved LiMn_2O_4

GUIYANG LIU*, KONG XIN, LILI ZHANG, BAOSAN WANG, YING HE

College of Science, Honghe University, Mengzi Yunnan, China 661100

Spinel LiMn_2O_4 has been synthesized by a glycerol-assisted combustion synthesis method. The phase composition and morphologies of the compound were ascertained by X-ray diffraction (XRD) and scanning electron microscope (SEM). The electrochemical characterization was performed by using CR2032 coin-type cell. XRD analysis indicates that single phase spinel LiMn_2O_4 with good crystallinity has been obtained as a result of 5 h treatment at 600 °C. SEM investigation indicates that the average particle size of the sample is 200 nm. The initial discharge specific capacity of the LiMn_2O_4 is 123 mAh/g at a current density of 30 mA/g. When the current density increased to 300 mA/g, the LiMn_2O_4 offered a discharge specific capacity of 86 mAh/g. Compared with the LiMn_2O_4 prepared by a conventional solution combustion synthesis method at the same temperature, the prepared LiMn_2O_4 possesses higher purity, better crystallinity and more uniformly dispersed particles. Moreover, the initial discharge specific capacity, rate capability and cycling performance of the prepared LiMn_2O_4 are significantly improved.

Keywords: *lithium ion batteries; cathode; spinel; solution combustion synthesis*

© Wrocław University of Technology.

1. Introduction

Spinel LiMn_2O_4 has been extensively studied in electrochemical field due to its potential use as a cathode material for lithium ion batteries. In comparison with the conventional LiCoO_2 cathode electrode, it is safer, cheaper, contains more common elements, and is environmentally friendly [1]. However, LiMn_2O_4 creates problems such as capacity fading and limited cyclability [2]. It has been found that LiMn_2O_4 possessing single-phase, high crystallinity as well as uniform and well-dispersed particle morphology has better electrode properties [3, 4]. LiMn_2O_4 powders have been synthesized by solid-state reaction method at high temperatures of 700 – 900 °C. This method has several disadvantages: inhomogeneity, irregular morphology and large average particle size with a broad particle size distribution, as well as poor control of stoichiometry, high temperature and long synthesis time [5, 6]. In order to solve such problems, several soft-chemical methods have been widely intro-

duced, such as sol-gel [7], freeze-drying [8] and the Pechini process [9]. Homogeneous spinel materials with small particle size can be synthesized by these methods. However, the preparation process is complicated and synthesis temperature is high (>700 °C).

Solution combustion synthesis is a simple and direct method to synthesize spinel LiMn_2O_4 [10, 11]. However, the purity and crystallinity of the powders prepared by this method at low temperature (<700 °C) is low, resulting in bad electrochemical performance. In order to get single phase LiMn_2O_4 with good crystallinity, high temperature and long synthesis time are needed. Yang et al. [12] and Lu et al. [13] reported that they employed a very long firing process of more than 10 h at the temperature >700 °C to get single phase LiMn_2O_4 . In addition, the conventional fuel urea is not in line with environmental standards, because nitrogen oxides are released in the combustion reaction.

In our previous works [14, 15], it was found that impurity formation could be attributed to the high combustion rate of the conventional solution syn-

*E-mail: liuguiyang@tsinghua.org.cn

thesis method, and the combustion rate was influenced significantly by the content of oxidizer (the main oxidizer in the system is NO_3^-). In this paper, in order to improve the disadvantages of the conventional solution combustion synthesis method, the method has been modified as follows: 1) Acetate salts have been used to substitute the nitrate ones partly, in order to decrease the combustion rate by decreasing the content of oxidizer. 2) Glycerol has been used as a new fuel. The structure, morphology and electrochemical performance of the prepared LiMn_2O_4 have been investigated in detail.

2. Experimental

2.1. Preparation

Firstly, 10 g raw materials of LiNO_3 (AR, 99 %), $\text{Mn}(\text{NO}_3)_2$ (AR, 99 %), CH_3COOLi (AR, 99 %) and $(\text{CH}_3\text{COO})_2\text{Mn}$ (AR, 99 %) with the mole ratio of 0.5:1:0.5:1 were dissolved in 5 ml 10 wt.% aqueous glycerol to obtain a solution. Then, the solution was put into a muffle furnace and was directly heated at 600 °C for 5 h. After cooling down to room temperature naturally in the muffle furnace, the product was obtained. As a comparison, a LiMn_2O_4 powder was also synthesized by the conventional solution combustion synthesis [12] under the same temperature and time, wherein the raw materials and fuel were LiNO_3 (AR, 99 %), $\text{Mn}(\text{NO}_3)_2$ (AR, 99 %) and urea. The initial materials were dissolved in distilled water.

2.2. Characterization

The phase composition and crystallinity of the samples were ascertained by X-ray diffraction (XRD, D/max-rB, diffractometer with $\text{Cu-K}\alpha$ radiation, $\lambda = 1.5406 \text{ \AA}$) within scattering angles of 10° and 70° in steps of 0.02°. The morphologies of the samples were observed by scanning electron microscope (SEM, XL30ESEM-TMP, Philips). Thermal decomposition behavior of the powders was examined by thermogravimetric analysis (TGA) and differential thermal analysis (DTA, Netzsch STA, Germany) at a heating rate of 10°/min under air.

2.3. Electrochemical performance test

The electrochemical characterizations were performed by using CR2032 coin-type cell. For LiMn_2O_4 electrode fabrication, the prepared LiMn_2O_4 powders were mixed with 10 wt.% of carbon black and 10 wt.% of polyvinylidene fluoride in N-methyl pyrrolidinone until slurry was obtained. Then, the blended slurries were pasted onto an aluminum current collector, and the electrode was dried at 120 °C for 12 h in vacuum. The test cell consisted of the LiMn_2O_4 electrode as cathode electrode, lithium foil as anode electrode, a porous polypropylene film as a separator and 1 M LiPF_6 in EC/EMC/DMC (1:1:1 in volume) as an electrolyte. The cells were assembled in an argon-filled glove box and cycled at room temperature. The electrochemical performances of the samples were evaluated upon cycling in the 3.2 – 4.35 V versus Li/Li^+ electrode.

3. Results and discussion

3.1. Phase composition

The XRD patterns of the products obtained by the conventional solution combustion (CC- LiMn_2O_4) and the glycerol-assisted solution combustion synthesis method (GC- LiMn_2O_4) are shown in Fig. 1(a) and Fig. 1(b). As shown in Fig. 1(a), the main peaks of CC- LiMn_2O_4 correspond to LiMn_2O_4 (JCPDS 35-0782). Some impurities peaks are found in the sample, which correspond to Mn_2O_3 . For GC- LiMn_2O_4 in Fig. 1(b), all the peaks are in good agreement with LiMn_2O_4 , indicating that a single phase LiMn_2O_4 is obtained. The temperature and time needed to obtain a single phase LiMn_2O_4 were only 600 °C and 5 h, which were lower than these parameters for the products prepared by the conventional solution combustion synthesis method reported in literature [11–13]. Noticeably, there is a substantial increase in the intensities from the peaks in Fig. 1(b) in comparison to the peaks in Fig. 1(a). This increase signifies a substantial increase in the crystallinity of GC- LiMn_2O_4 . Because the combustion rate in the glycerol-assisted combustion system was decelerated by decreasing the content of

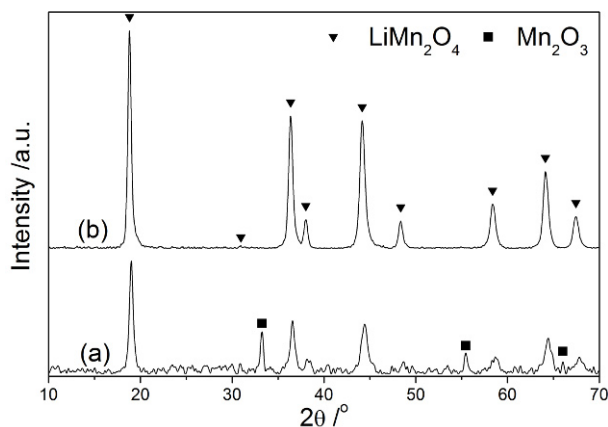


Fig. 1. XRD patterns of (a) CC-LiMn₂O₄ and (b) GC-LiMn₂O₄.

oxidizer (NO₃⁻), and glycerol was able to release more heat than that of urea [16] in the combustion system to accelerate the formation of LiMn₂O₄, the purity and crystallinity of GC-LiMn₂O₄ could be well improved.

3.2. Thermal characteristics and micro morphology.

Fig. 2 shows the TG/DTA patterns of CC-LiMn₂O₄ and GC-LiMn₂O₄. The weight change has not exceeded 2% for both the powders between 100 and 900 °C, suggesting stable thermal characteristics. For CC-LiMn₂O₄, the LiMn₂O₄ may be further generated from the impurity Mn₂O₃, resulting in a little weight change (<0.6%). For GC-LiMn₂O₄, there was a minor weight increase (<2%) between 100 and 900 °C, corresponding to the further oxidation of LiMn₂O₄ [13]. DTA analysis revealed minor endothermic change for CC-LiMn₂O₄ and a little exothermic change for GC-LiMn₂O₄, corresponding to the TG curves of CC-LiMn₂O₄ and GC-LiMn₂O₄, respectively.

The SEM surface morphologies of the products prepared by the two methods are shown in Fig. 3. The particles of CC-LiMn₂O₄ in Fig. 3a are not uniform and badly agglomerated. In contrast, the particles of GC-LiMn₂O₄ in Fig. 3b and Fig. 3c are uniform and well dispersed. The average particle size of GC-LiMn₂O₄ is ~200 nm.

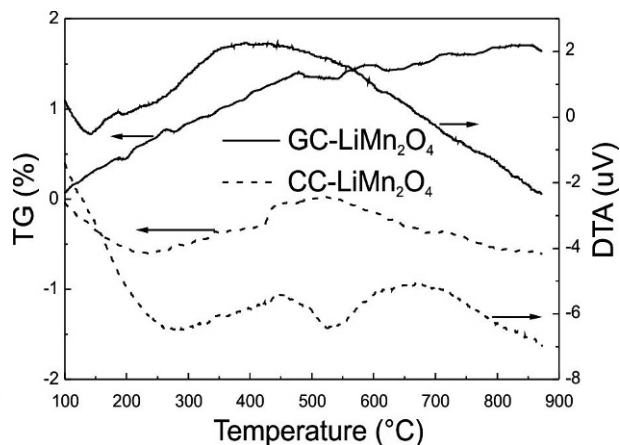


Fig. 2. TG/DTA curves of CC-LiMn₂O₄ and GC-LiMn₂O₄. The test was performed at a heating rate of 10 °/min in the temperature range of 100 – 900 °C under air.

3.3. Electrochemical performance.

The initial discharge curve in Fig. 4 shows two plateaus at 4.1 V and 3.9 V, which is a typical profile of LiMn₂O₄ [17]. The initial discharge specific capacity and coulomb efficiency of GC-LiMn₂O₄ are 123 mAh/g and 92.9%, respectively. They are much higher than these of 81 mAh/g and 87.8% for CC-LiMn₂O₄. Moreover, the lower charging plateau and higher discharging plateau of GC-LiMn₂O₄ demonstrates that the electrochemical performance of GC-LiMn₂O₄ is superior to that of CC-LiMn₂O₄ [18].

The discharge curves at various current densities in Fig. 5 show that the rate capability of GC-LiMn₂O₄ (Fig. 5(b)) is superior to that of CC-LiMn₂O₄ (Fig. 5(a)). GC-LiMn₂O₄ retains much higher capacity at high rates than CC-LiMn₂O₄ does. Even at the current density of 300 mA/g, GC-LiMn₂O₄ offers a discharge specific capacity of 86 mAh/g. But for CC-LiMn₂O₄, the discharge specific capacity is only 42 mAh/g at a current density of 150 mA/g. Cycling performances of the two samples shown in Fig. 6 demonstrate that the cycling performance of GC-LiMn₂O₄ is better than that of CC-LiMn₂O₄. The discharge specific capacity of GC-LiMn₂O₄ retains 82% after 100 cycles, whereas the discharge specific capacity of CC-LiMn₂O₄ retains only 81% after 30 cycles. It has been found that capacity and

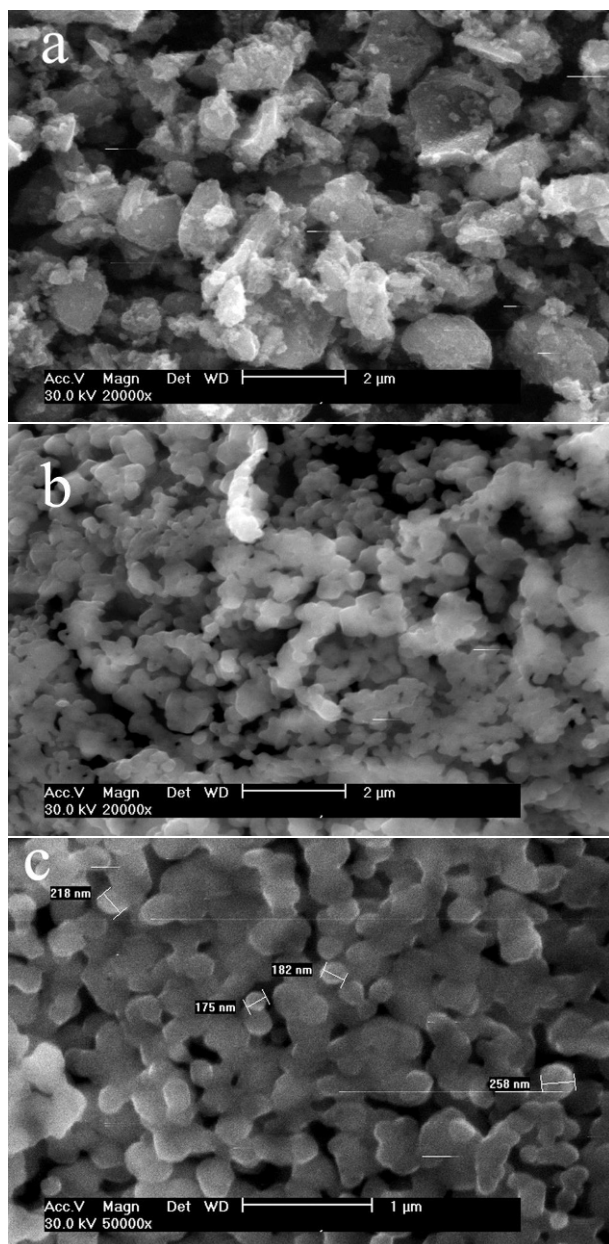


Fig. 3. SEM morphologies of (a) CC- LiMn_2O_4 , (b) and (c) GC- LiMn_2O_4 .

cycling performance can be improved by enhancing the purity and crystallinity of LiMn_2O_4 [19], and rate capability can be enhanced by obtaining sub-micron and well dispersed particles [20]. GC- LiMn_2O_4 presented in this paper has high purity, good crystallinity as well as sub-micron uniformly dispersed particles therefore it exhibits improved electrochemical performance.

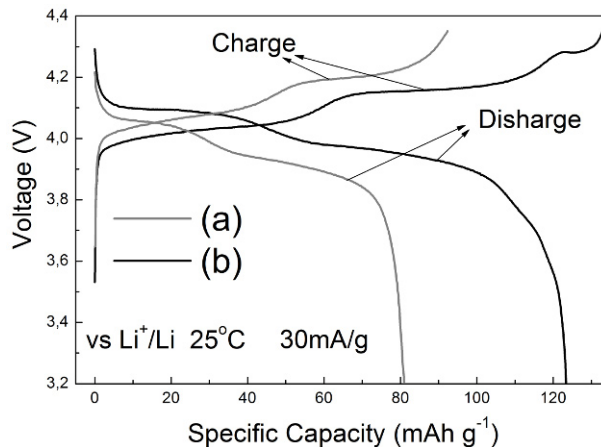


Fig. 4. Initial charge/discharge curves of (a) CC- LiMn_2O_4 and (b) GC- LiMn_2O_4 at 30 mA/g within the voltage window of 3.2 – 4.35 V versus metal Li. The test was performed in a constant current and constant voltage mode. The cell was charged with a constant current (30 mA/g) to 4.35 V, held at 4.35 V for 1 hour and discharged at a constant current (30 mA/g) to 3.2 V.

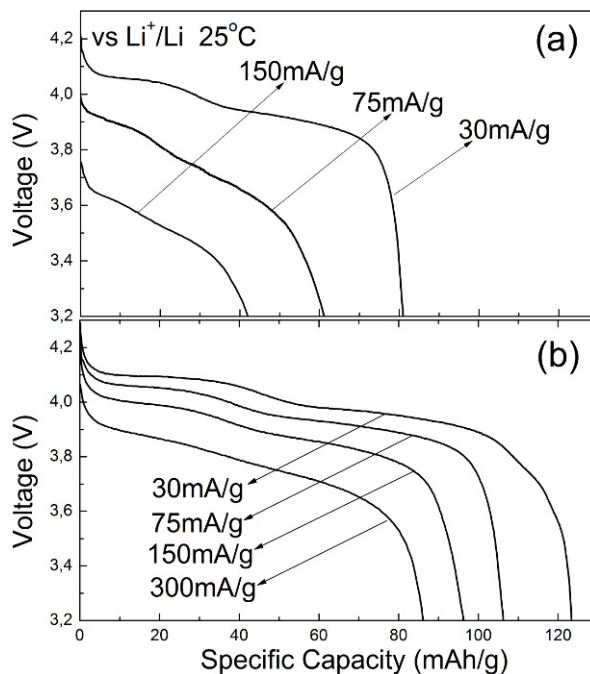


Fig. 5. Discharge curves at various current densities for (a) CC- LiMn_2O_4 and (b) GC- LiMn_2O_4 at various current densities within the voltage window of 3.2 – 4.35 V versus metal Li. The test was performed in a constant current and constant voltage mode.

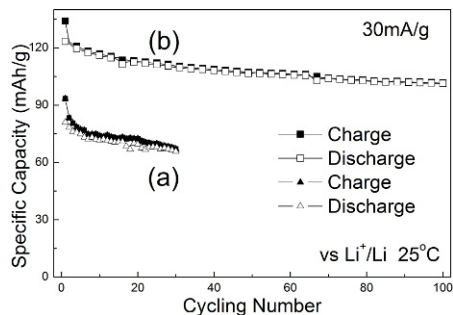


Fig. 6. Cycling performance of (a) CC-LiMn₂O₄ and (b) GC-LiMn₂O₄ at 30 mA/g in a constant current and constant voltage mode. The cycling performance was evaluated by using specific discharge capacity as a function of cycle number.

4. Conclusions

Single phase spinel LiMn₂O₄ with good crystallinity has been synthesized by a glycerol-assisted combustion synthesis at 600 °C for 5 h. Compared with the product synthesized by the conventional solution synthesis method at the same temperature and time, the purity, crystallinity and micro morphology, as well as the initial discharge specific capacity, rate capability and cycle performance of the prepared product are greatly improved.

Acknowledgements

The present work was supported by the National Natural Science Foundation of China (No.51062018), Natural Science Foundation of Yunnan Province (2012FB173) and the Key Subject of Materials Physics and Chemistry of Honghe University.

References

[1] LIU W., KOWAL K., FARRINGTON G.C., *J Electrochem Soc.*, 145 (1998), 459.

- [2] HUANG H., VINCENT C.A., BRUCE P.G., *J Electrochem Soc.*, 146 (1999), 481.
- [3] AMATUCCI G.G., PEREIRA N., ZHENG T., TARASCON J.M., *J Electrochem Soc.*, 148 (2001), A 171.
- [4] HON Y.M., LIN S.P., FUNG K.Z., HON M.H., *J Eur. Ceram. Soc.*, 22 (2002), 653.
- [5] WU H.M., TU J.P., YUAN Y.F., LI Y., ZHAO X.B., CAO G.S., *Mater. Chem. Phys.*, 93 (2005), 461.
- [6] SUN Y., WANG Z., CHEN L., HUANG X., *J Electrochem Soc.*, 150 (2003), A1294.
- [7] HWANG B.G., SANTHANAM R., LIU D.G., *J Power Sources*, 101 (2001), 86.
- [8] ZHECHEVA E.N., GOROVA M.Y., STOYANAVA R.K., *J Mater. Chem.*, 9 (1999), 1559.
- [9] LIU W., FARRINGTON G.C., CHAPUT F., DUNN B., *J Electrochem Soc.*, 143 (1996), 879.
- [10] CHITRA S., KALAYANI P., MOHAN T., *J Electrochem.*, 3–4 (1999), 433.
- [11] LEE K.M., CHOI H.J., LEE J.G., *J Mater. Sci. Lett.*, 20 (2001), 1309.
- [12] YAGN W.S., ZHANG G., XIE J.Y., *J Power Sources*, 80–82 (1999), 412.
- [13] LU C.Z., FEY G.T.K., *J Phys. Chem. Solids*, 67 (2006), 756.
- [14] LIU G.Y., GUO D.W., GUO J.M., *Key Eng. Mater.*, 368–372 (2008), 293.
- [15] LIU G.Y., GUO J.M., WANG B.S., *Adv. Mater. Res.*, 143–144 (2011), 125.
- [16] DEAN J.A. *Lange's Chemistry Handbook*, McGraw-Hill Publisher, New York, 1999.
- [17] ARIYOSHI K., IWATA E., KUNIYOSHI M. et al., *Electrochem. Solid ST*, 9 (2006), 337.
- [18] FANG H., LI L.P., YANG Y., *J. Power Sources*, 184 (2008), 494.
- [19] KALYANI P., KALAISELVI N., MUNIYANDI N., *J. Power Sources*, 111 (2002), 232.
- [20] FERGUS J.W., *J. Power Sources*, 195 (2010), 939.

Received 2012-09-28

Accepted 2013-04-22